GLL
Geomatics, Landmanagement and Landscape No. 4 • 2022, 109–122

EVALUATION OF THE CAPABILITIES OF SATELLITE IMAGES ALSAT 2-A FOR EMERGENCY MAPPING IN URBAN AREAS, CASE OF THE CITY OF M'SILA (ALGERIA)

Tarek Medjadj, Hayet Ghribi

Summary

In this paper, we will show the capabilities and limitations of Alsat-2 images in mapping urban areas in emergency situation. The aim of the research was to provide urban information that is geo-referenced in real time during natural disasters (floods, earthquakes). It's important for fast decision-making so that they will be a necessary support for the estimation of the damages. The following study tests the spatial and radiometric quality of Alsat 2-A images and proposes technical solutions for theiruse in urban mapping.
In order to identify and extract the ground realities, we shall describe and make an effort to discern the perceptible aspects of features in urban area. The adopted methodology carries out a statistical analysis of the information extracted from Alsat-2 images of the studied area (the city of M'Sila, Algeria) using classification and segmentation methods. The statistics will show the percentage of the area in relation to the total size of geometric surface and the distance for linear objects. As a result, the quality of the extracted urban texture necessary for urban mapping will be determined. Image processing to improve resolution quality was carried out using merging method. However, the analysis of consistency and discrepancy of these statistics will be done by comparing samples of field data using confusion matrix.

Keywords

urban mapping • Alsat-2A • image processing • disaster management

1. Introduction

The lack of high spatial resolution imagery prior to 1997 is the main reason for insufficient research on remote sensing in urban areas. Since then, a variety of processes have been covered in multiple studies using high-resolution imagery [Dubois et al. 1997, Shan Yu et al. 1999, Donnay et al. 2000]. With the emergence of very high-resolution satellite imagery (Ikonos, Quickbird, OrbView, Cartosat, Spoot 5), great efforts have been made in the related fields of urban remote sensing [Puissant and Weber 2003, Bhatta et al. 2010, Van der Kwast et al. 2011, Weng 2012, Armand 2016, Brown and McCarty 2017, Leichtle et al. 2017]. In Algeria, the National Institute

of Cartography and Remote Sensing has adopted "two scales [that] were used for the base mapping: 1/50 000 for the northern part, which covers one fifth of the area of Algeria and 1/200 000 for the entire national territory. The base map 1: 50,000 was produced from the photogrammetric restitution of aerial photographs at scale 1: 64,000" [Haddanou 2005]. However, the priority was to complete the base maps for the entire territory of Algeria, particularly, the northern parts of the country. Recently, a new satellite was launched that uses high resolution spatial satellite imagery for mapping at finer scales including the production of space maps and base map. The satellite Alsat-2A was launched by the Algerian Space Agency (ASAL) in 2012. It has not yet been explored in urban studies except the papers published by Medjadj [2018] and Ourabia et al. [2016]. The availability of high resolution images of urban areas gives an opportunity to explore remote sensing for urban mapping more. These images disrupt our understanding of the complexity of urban space, and they have a capability of achieving good spatial and spectral resolution. This will open a new perspective in analysing the problems of urban spaces. We have already seen, in the case of Algerian cities, "a significant heterogeneity of urban forms, objects size and their spatial organisation due to the context of rapid urbanisation combined with the urban anarchy inherited from several planning models" [Medjadj 2018]. In the city of M'Sila (the area of study), there are several neighbourhoods experiencing flooding problems, often located on the side of a water stream, or even in a riverbed, while lacking any rainwater catchment system. In the region of Hodna (2007, 2019) there are a lot of rainstorms that cause enormous damage, both material or human. Knowing "that 1066 000,00 DA is the investments committed to the fight against floods in wilaya of M'Sila in 2018/2019" [MRE 2019]. To minimise the risk of damages due to flooding in the city of M'Sila, we study the high spatial resolution images to produce maps for use in risk prevention and risk management (post-disasters). Our study does not only concern the extraction of feature objects from Alsat 2-A images but also the production of structured information that will be interoperable with GIS. The time factor is taken into account, therefore our estimates are based on quality tests and on the time required to meet the conditions and needs of risk prevention/management. The impervious surface has an important role in the process of collecting rainwater in the city of M'Sila. "Location, geometry and spatial patterns of impervious surfaces, and the previous-impervious surface ratio […] have a hydrological impact" [Weng 2012]. However, it does not indicate only surface objects (such as buildings) but also linear objects. In the case of high-resolution images, linear objects in urban space will have one breadth and they had a surface (such as streets). Therefore, in our case we will concentrate on the extraction of the impervious surface, with less emphasis on interpretations of the urban features. Information on impervious surfaces is extremely important for urban planning, and particularly for rainwater harvesting. They could also be an indicator in the ranking of flood zones in the city of M'Sila.

Several techniques have been applied for mapping at the urban scale (photogrammetric method, Radar, Lidar). The data quality depends on the performance of the techniques were used. The Global Positioning System (GPS) could also provide valu-

able information on this subject, but at a high costs and a long time. In the past, operators have used digitalisation from aerial photographs to retrieve information from the ground. Recently, there have been new development sin algorithm-based automatic extraction methods. These were the results of research that were carried out in the field of urban mapping from high spatial resolution satellite imagery [Puissant and Weber 2003, Shen et al. 2011, Benza et al. 2016, Taubenböck et al. 2017, Zhu et al. 2018].

2. Study area and data source

2.1. Area of interest

M'Sila is a medium-sized city in Algeria. It covers an area of 18,175 km^2 with an estimated population of 1,210,952 inhabitants, an average density of 66 inhabitants/km^2 [RGPH 2008]. The population growth rate of the wilaya of M'Sila is estimated at 2.1%/year between 2008 and 2022, according to the national statistics office.

The studied area is part of the municipality of M'Sila, and includes the land use of the city and land cover of the whole space covered by the Alsat 2-A image scene (Cf. Fig. 2). Located between two viewing circles: '35.48°, '35.67° north of the equator and linear length: '4.57°, '4.48° east of Greenwich line (Cf. Fig. 1).

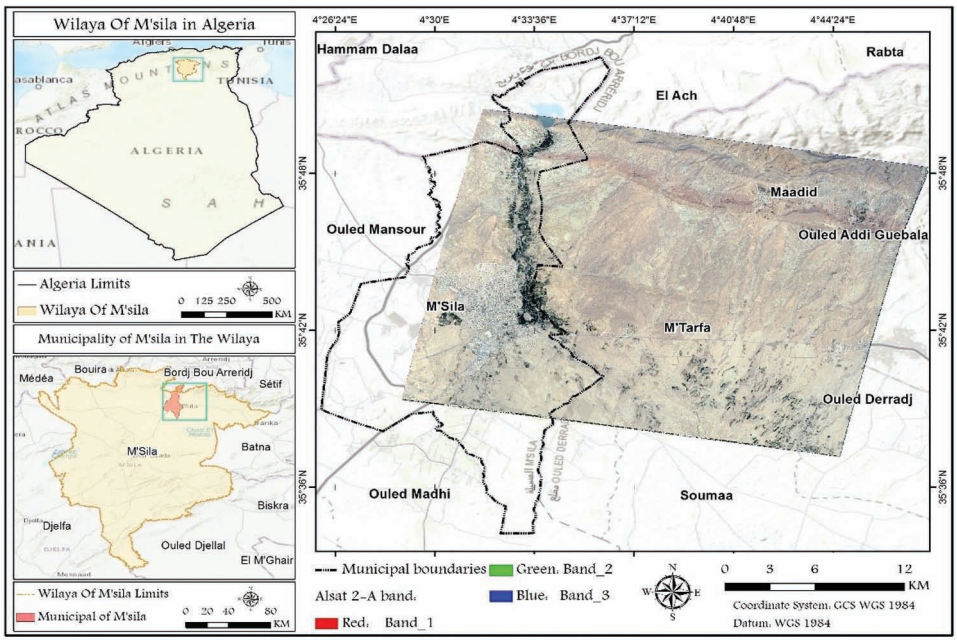

Source: Authors' own study

Fig. 1. Location of the study area

The city of M'Sila is located in the Hodna Region. It is characterised by a semi-arid climate with precipitation of around 400 mm/year, according to data from the national meteorological office. The topography of the area is homogeneous with vast plains crossed by small hills. The vegetation cover is not dense and is characterised by small plants in theform of breedingpastures.

2.2. Data source and software

The ALSAT-2A satellite provides two types of images, panchromatic (PAN) and multi-spectral (MS). We have used both types of images (PAN/MS) to cover the study area. Each kind of images is different in terms of radiometry and spatial resolution:

PAN mode: 2,5 m with spectral band: 0,45–745 μm
MS mode: 10 m with spectral band (04 bands)

- B1: 0.45–0.52 μm (Blue),
- B2: 0.53–0.59 μm (Green),
- B3: 0.62–0.69 μm (Red),
- B4: 0.76–0.89 μm (Near Infrared).

Swath of Both scene elementary (PAN/MS): 17.5 km × 17.5 km (306.25 km^2)

There are several software packages for processing satellite imagery that have significant potential and capabilities in terms of analysis. We have used the *Orfeo toolbox* under the *Qgis* open source which offers advanced functionalities and allows access to the sources of the programs to run and even improve the algorithms if necessary. Our choice was motivated by the analysis and processing capabilities providedby this software as well as bythe possibilitiesrelated to the rights of use as open source.The entire mapping process, whichwe called "Map chain", could be done with the *Qgis* and the *Orfeo* module. No other softwarecould do this task on its own. We have to use two types of software, one to processthesatellite images (remote sensing) and the other to processthe retrieved vector data (GIS).

3. Materials and methods

The applied scale of mapping and spatial resolution of images are interdependent. However, identifying urban features comes a san in convenience that is related, in particular, to the accuracy (the tolerance of geometric error) and the shadows generated by the buildings. Lhomme [2005] tried to propose a solution to this problem by developing an extraction method for buildings after a strict formalisation of objectives of approach based on textural building definition. In the following, additional information (such as shadows and vegetation) are integrated to reduce commissions errors. The shadow casted by buildings, often generated by the angle of the solar incidence, is a visual noise of an image. The height of buildings in the majority of collective housing areas of the city of M'Sila does not exceed 5th floors. The reason for this is a directive of the master plan for development and urban planning (PDAU) and the land use plan (POS). So, the effect of the high building will have no impact on our case, especially,

if we choose the optimum moment for the shooting. In fact, the angle of incidence of electromagnetic radiation during the shooting must be taken into account to minimise the shadow cast by buildings which could obscure impervious surfaces (roadways and sidewalks). "Distortions in the shadows cast by buildings can also affect the accuracy and quality of urban information, as urban streets can be misclassified as vegetation, leading to an error rate of 30%" [Van der Linden and Hostert 2009].

The extraction of urban structures and objects, whether linear or planar, is a very active research area due to the usefulness of the information obtained for risk management and the study of changes in land use. In particular, several methods have been developed based on mathematical morphology approaches [Mohammadzadah et al. 2006, Benblidia et al. 2006], the pre-exile classification of images [Zhang et Lin 2010, Matgen et al. 2011, Zhu et al. 2018] and segmentation [Michel 1988].

After a review of the main methods used for the identification and extraction of urban objects it should be noted first that Puissant and Weber [2003] has conducted an interesting research for the detection of geographic information compared to the spatial resolution of satellite images. They arrive at the threshold of detection of optimal geographic objects (Cf. Table 1).

Table 1. The detection threshold of spatial objects of optimal spatial resolution

Objects	Optimal spatial resolution
Square objects with circular pavilions, individual trees	0.8 to 1 m
Linear objects, such as roads	1 to 2 m
Rectangular objects, such as square buildings	2 to 3 m
Areas of any shape type, vegetation zone	6 to 8 m

Source: Puissant and Weber [2003].

The analysis of Table 1 already shows the limits of Asat 2-A images (MS) that a spatial resolution of 10 m. Therefore, it is not sufficient for the identification of ground features in urban areas, as shown in Fig. 3: subset (a). Therefore, we thought of using the merging method to improve the quality of multispectral images (MS). It will be merged with a panchromatic image which has a resolution of 2.5 m as shown in Figure 3: subset (b). As a result, we will obtain a new merged multispectral image with a resolution of 2.5 m. The value of the panchromatic channel is proportional to the integrated correlation it has with the multi-channel spectrum, using the following equation [Ranchin and Wald 1995]:

$$PIn\ (x, y) = [(Muln\ (x, y) \cdot (1 - Coefn))\ Pan\ 2 + (x, y) \cdot (1 - Coefn)\ 2]\ ½ \qquad (1)$$

where:

PIn – pixels resulting from the integration of Muln and panchromatic,
n – channel number,

Muln – numerical value of the pixel (x, y) of the n-channel multi-spectral image,
Coefn – correlation coefficient for the panchromatic channel with *Muln* channel.

Secondly, we will apply the classification and segmentation methods to perform tests on the Aalst 2-A images that were previously merged. At the end of each process we have to identify the urban features. An exhaustive list of all georeferenced details will be presented as the percentage of the total studied area. This test will be followed by a statistical analysis of the details of the extracted features. Also, the purpose of this stage of research is to create a table for a comparison between three cases of image processing applied to each subset of area of interest. Therefore, the characteristics and specificities of the form and size of urban objects will be described in order to certify the detection capability for each type of urban features. The statistics will then be presented as the percentage of areas in relation to the total size of the natural and geometric surface themes, and as the distance in kilometers for linear themes. These statistics will be examined in the next stage.

Finally, an analysis of the consistency and discrepancy of these statistics will be run to validate the accuracy of the results. At this stage, we have planned to calculate a statistical index called the *Kappa index*. This index is used to select the best result according to the methods used to extract data. It will be calculated from the information of the *confusion matrix* where the rows are reserved for the observation data (data field) and the columns for the extracted data. It is therefore a quality estimator which takes into account errors in rows and columns. Its value is between 0 and 1.

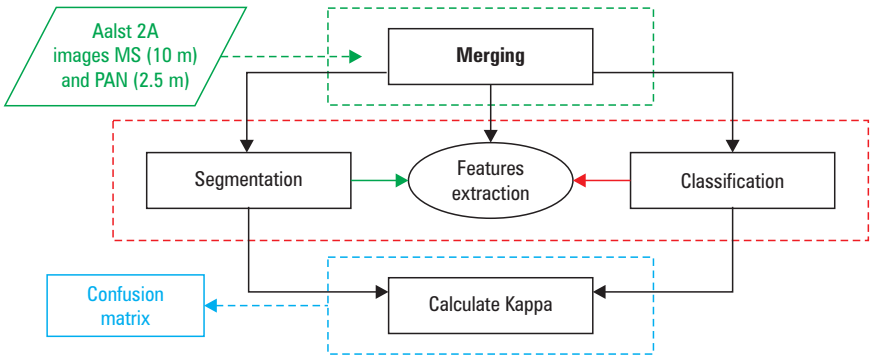

Source: Authors' own study

Fig. 2. Methodology flowchart

4. Results and discussion

4.1. Which resolution for which needs?

In order to definethe experimental protocols, the scientific user simply has to find the treatment that best suits his expertise and the objective he has set. We have planned

a reprocessing chain of two images, raw multispectral and panchromatic satellite images. This chain starts with the radiometric correctionof the multispectral image and the geometric corrections of both images. These two images are superimposed and merged, in order to exploit the advantages of each of them. The multispectral image offers a better radiometric resolution to the radiometric classification, which is very useful, while the panchromatic image givesa better spatial resolution to discriminate urban objects.

In the following (Cf. Fig. 3), a subset of images which represents the spatial quality before / after processing with the "Merge" option ($a + b = c$).

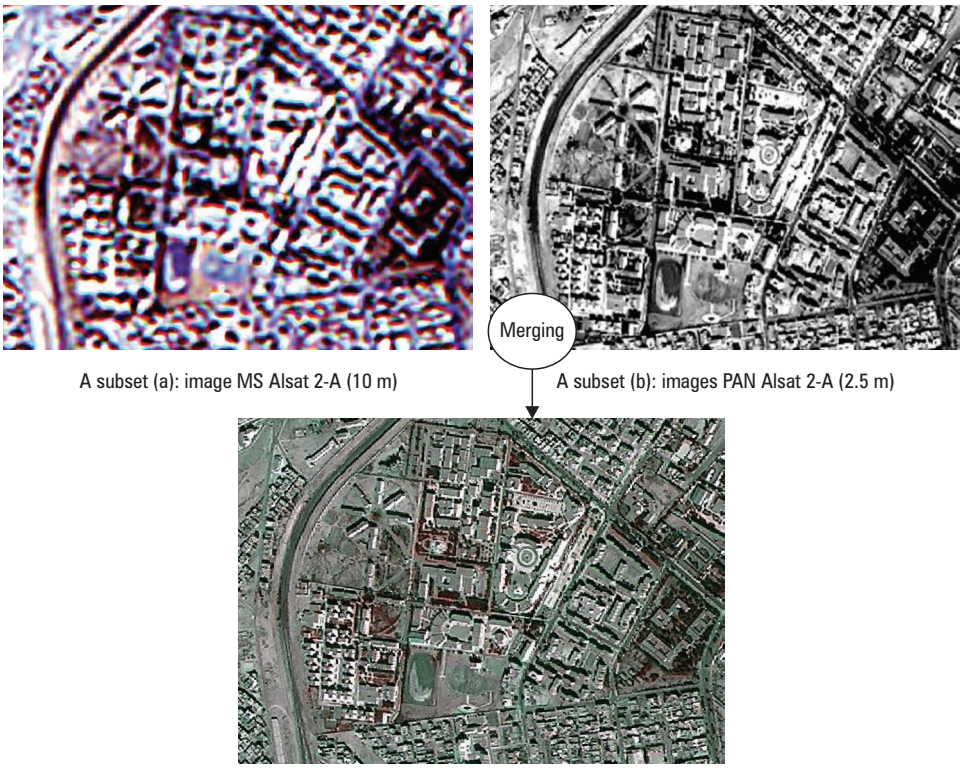

Source: Authors' own study

Fig. 3. Merging process between MS and PAN Alsat 2-A images

"The lack of information on urban areas is the main inconvenience in facing and managing floods as 92% of the risk in cities" [UNSD 2022]. In our case, we focus on the geographic information need related to the emergency mapping of urban space. Before doing so, we will estimate the number of features extracted from a sample of urban areas and also examine the quality obtained by the images we use (Cf. Table 2).

Table 2. Accuracy of urban objects in the Alsat2-A image

	MS (10 m)	PAN (2.5)	Merged (MS: 2.5 m)
Built-up	impossible	difficult	easy
Street	easy	easy	easy
Road	impossible	difficult	easy
Vegetation	difficult	impossible	easy
Soil	impossible	difficult	difficult
Impervious surface	impossible	difficult	difficult
Stream	impossible	impossible	difficult
Bridge	impossible	easy	difficult

As shown in Table 2, the identification of several objects (building, road, impervious surface, bridge) is difficult or almost impossible, especially in the MS and PAN images. When the images were merged (MS/PAN), we have obtained a better result but not sufficient some objects. However, the new, merged image in more capable of detecting objects, thus should be useful for easy extraction of buildings, streets, roads and vegetation. Elsewhere, it was difficult to identify other features such as soil, impervious surfaces, stream and bridges. Therefore, we can confirm that the merged image with spatial resolution of 2.5 m is insufficient for urban mapping in the case of city of M'Sila where the urban area is characterised by a high density. It's difficult to identify the features necessary for mapping urban disasters like floods, since such mapping requires more information about impervious surfaces, streams and bridges. The visual perception is not sufficient to extract data in a very short time that is necessary in urban disasters. So, to solve this problem, we will perform image processing with classification and segmentation methods to improve the quality of identification and extraction of urban features whose quality is not sufficient, as was shown in Table 2.

4.2. Output of classification method

We have done the supervised classification of K-means options in the studied area (subset c). The results of processing have been presented in Figure 4.

Urban areas are described by morphological aspects, usually using typo-morphological method analysis. Otherwise, the use of multi-spectral data with classification method leads to zonal descriptions of the urban space and is usually limited to the land or zonal descriptions of building densities [Gadal et al. 2012]. The shadows of the buildings are identified and classified as ground, especially in the case of unsupervised classification. To avoid this misclassification, we have created a "shadow" class with the supervised classification method, and we obtained images classified separately. We

use it for filtering process to eliminate the noise caused by shadows. At the end of this process, we can distinguish three (3) groups of features as shown in Figure 4:

- Features that are identifiable due to good quality like asphalt and ground (brown colours) but it's difficult to distinguishing between this two types of objects.
- Features which are significant in identifying objects such as vegetation (green colour), but the contours of large vegetation areas are not clear and presented with low accuracy. Urban vegetation is detectable but it is not possible to distinguishing between trees and interstitial plant areas.
- Objects that are difficult to identify and that have contours that separate them from other neighbourhood features. Therefore, they can only be identified in scattered urban areas.

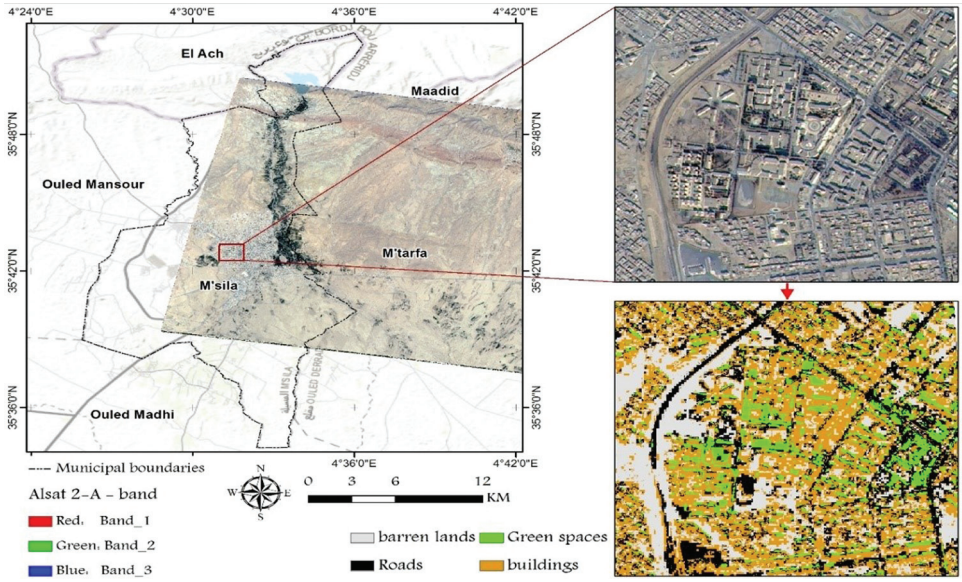

Source: Authors' own study

Fig. 4. Supervised classification of subsets image (c)

4.3. Accuracy assessment of classification

This step consists in calculating the *Kappa index*. This index will be used to validate the results of classification and to evaluate the reliability of the map presented in Figure 4. It is calculated from the information provided by the confusion matrix, the lines of which correspond to field observation data and the columns to classification data. We can also calculate the error mask images for each class showing which pixels were incorrectly classified. To calculate this index, we have generated a point layer with the Qgis software whose points are distributed randomly over the studied area. We have

defined a total of 200 points by assigning a number of points to each class (Cf. Table 3). The points are filled according to the information from the image. We performed an intersection operation of this layer with the one resulting from the classification to obtain a layer in which the points are assigned to their land use class. Using an SQL query under GIS, the data of the confusion matrix was informed as shown in Table 3.

Table 3. Confusion matrix (image *c*)

		Classification							
		1	**2**	**3**	**4**	**5**	**6**	**Total**	**Producer Accuracy**
Field data	**1**	45	0	0	0	0	0	45	**100%**
	2	1	7	0	1	0	1	10	**70%**
	3	6	0	11	1	0	3	21	**52%**
	4	0	0	2	18	12	6	38	**38%**
	5	1	0	1	1	32	8	43	**68%**
	6	5	0	5	5	9	19	43	**46%**
Total		58	7	19	26	53	37	200	
User Accuracy		77%	100%	59%	68%	58%	56%		
Global accuracy : 69 % **Kappa index:** 0,6									

Explanations: **1.** Impervious surface, **2.** water, **3.** soil, **4.** built-up, **5.** gardens and lawns, **6.** vegetation

We obtained an index value of 0,6 for the classification of the image (*c*). The global accuracy was also provided by the ratio between the number of well-classified pixels and the total number of pixels of the observations. Its value is 69%, which means that there is a moderate agreement between the classification and our verification data.

The results from the land cover layer show an agreement with the field data. The "impervious surface" class is close to 100%, and is followed by other classes, namely "water" (70%), "soil" (52%) and "built-up" (38%). The "built-up" class is difficult to classify as it interferes with other classes, knowing that the geometric shape is not taken into consideration in the classification. The vegetation cover is also difficult to define (Cf. Table 3).

4.4. Segmentation

We have carried out the segmentation with the Mean-Shift options. The results of processing have been presented in Figure 5.

Segmentation method is more effective for extraction of surface features with contours. The result of feature extraction will be saved in vector format as is shown in Figure 5. However, it's easy to use GIS software to improve the quality of data using geometric

correction tools. The scale parameters used have been determined in order to segment the objects very finely. This is the case for the "impervious surface" class, which includes objects with similar radiometric behaviour (asphalt, soil). We did the same for other objects, usually to determine their shape and compactness. We found it interesting to use the index values serving to best segment objects according to their shape and reflectance.

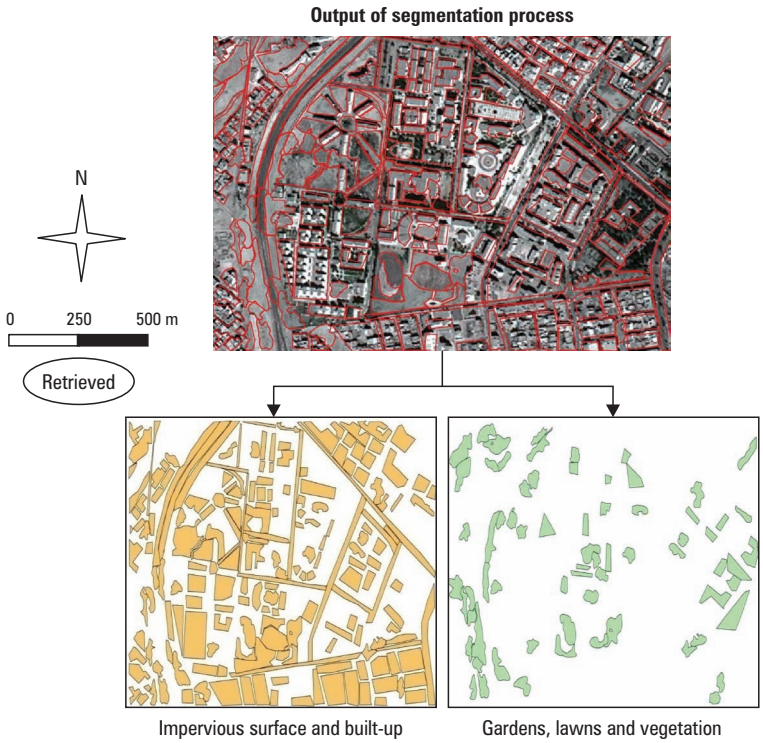

Fig. 5. Vector data retrieved from a subset of merging image (c)

5. Conclusion

The aim of this study was to identify features that could be used for emergency mapping in urban areas. We have examined the Alsat 2-A satellite images by visual perception, the identification of several objects (buildings, roads, impervious surfaces, bridges) was difficult or almost impossible. We then made an attempt at improving the quality of resolution using the merging method. However, the results obtained are better after the classification and segmentation process. These processes have enabled us to extract important surfaces of land use like impervious surfaces, built-up areas, water areas and soil. However, some imperfection have been detected, in particular due to the confusion between some classes with very similar characteristics (such as impervious

surfaces and soil). Also, we have observed a distortion of the shape of urban objects such as buildings. We applied the segmentation method to solve this problem and the results show a satisfactory quality of restitution. We estimate that the time of production by Victor data is acceptable (max. 2 hours for the entire map chain). This was the main point of our study, and it will be an interesting factor for fast decision-making in the case of emergency disaster.

Nowadays, urban mapping is not limited only to the analysis of the classification and segmentation of satellite images. This perspective can be supplemented by the analysis of spatial metrics to quantify and qualify shapes of urban objects with accuracy. The calculating of spatial metrics can be done using other specific indices.

Acknowledgements

The authors would like to thank Algerian Space Agency (ASAL) for supporting this work and providing the satellite images Alsat 2-A for free.

References

Armand M. 2016. Images satellitaires et planification des villes du Tiers-Monde. Mondes en développement, 176(4), 169. https://doi.org/10.3917/med.176.0169

Benblidia et al. 2006. Utilisation de la morphologie mathématique pour l'analyse de l'occupation de l'espace en zones urbaines et périurbaines présahariennes: cas de Laghouat (Algérie), Semantic Scholar (s.d.). Consulté 9 avril 2020. https://www.semanticscholar.org/paper/UTILISATION-DE-LA-MORPHOLOGIE-MATH%C3%89MATIQUE-POUR-DE-Benblidia Abdellaoui/ 1babe534de3f5a693287c66572d43beb593de31f

Benza M., Weeks J.R., Stow D.A., López-Carr D., Clarke K.C. 2016. A pattern-based definition of urban context using remote sensing and GIS. Remote Sensing of Environment, 183, 250–264. https://doi.org/10.1016/j.rse.2016.06.011

Bhatta B., Saraswati S., Bandyopadhyay D. 2010. Urban sprawl measurement from remote sensing data. Applied Geography, 30(4), 731–740. https://doi.org/10.1016/j.apgeog.2010.02.002

Blaschke T. 2009. Object based image analysis for remote sensing. ISPRS Journal of Photogrammetry and Remote Sensing.

Brown M., McCarty J. 2017. Is remote sensing useful for finding and monitoring urban farms? Applied Geography, 80, 23–33. https://doi.org/10.1016/j.apgeog.2017.01.008

Delavaud A. 2000. L'apport des images satellitaires dans l'étude des dynamiques de l'occupation du sol des villes d'Amérique Latine. Cybergeo. https://doi.org/10.4000/cybergeo.722

Donnay J.-P., Barnsley M.J., Longley P.A. (eds.). 2000. Remote Sensing and Urban Analysis: GISDATA 9. CRC Press. https://doi.org/10.1201/9781482268119

Dubois J.-M., Donnay J.-P., Ozer A., Boivin F., Lavoie A. 1997. Télédétection des milieux urbains et périurbains. AUPELF-UREF. https://orbi.uliege.be/handle/2268/20540

Gadal S., Gilg J.P., Biraud I. 2012. Caractérisation des zones urbaines par télédétection spatiale. IX èmes Journées du Réseau Télédétection, AUF.

Haddanou M. 2005. Les spécifications cartographiques en usage à l'INCT. Le bulletin interne de l'Institut National de Cartographie et de Télédétection, édition spéciale, 3, 15.

Hossain M.D., Chen D. 2019. Segmentation for Object-Based Image Analysis (OBIA): A review of algorithms and challenges from remote sensing perspective. ISPRS Journal of Photogrammetry and Remote Sensing, 150, 115–134. https://doi.org/10.1016/j.isprsjprs.2019.02

Hrvatin M., Perko D. 2003. Surface roughness and land use in Slovenia/Razgibanost površja in raba tal v Sloveniji. Acta Geographica Slovenica, 43-2. DOI: https://doi.org/10.3986/AGS43202

Kourgli A., Belhadj-Aissa A. 2003. Segmentation texturale des images urbaines par le biais de l'analyse variographique. Télédétection, 337–348.

Leichtle T., Geiß C., Wurm M., Lakes T., Taubenböck H. 2017. Unsupervised change detection in VHR remote sensing imagery – an object-based clustering approach in a dynamic urban environment. International Journal of Applied Earth Observation and Geoinformation, 54, 15–27. https://doi.org/10.1016/j.jag.2016.08.010

Lhomme. 2005. Identification di bâti à partir d'images satellitaires à très haute résolutions spatiales, thèse de doctorat en télédétection. Université de Sherbrooke, Canada.

Matgen P., Hostache R., Schumann G., Pfister L., Hoffmann L., Savenije H.H.G. 2011. Towards an automated SAR-based flood monitoring system: Lessons learned from two case studies. Physics and Chemistry of the Earth. Parts A/B/C, 36(7), 241–252. https://doi.org/10.1016/j.pce.2010.12.009

Medjadj T. 2018. Vers une nouvelle approche pour calculer les indicateurs de la densité urbaine via l'imagerie de satellite Alsat-2A. Bulletin des sciences géographiques, 36–43.

Messier N., Cavayas F., André P. 2001. Cartographie de l'occupation du sol en milieu urbain à partir d'images satellites de haute résolution spatiale, le cas de Beijing (Chine).

Michel A. 1988. (PDF) Segmentation et classification sur une image satellite SPOT en milieu urbain: Application à la ville de Quito (Equateur). Research Gate. https://www.researchgate.net/publication/32982700_Segmentation_et_classification_sur_une_image_satellite_SPOT_en_milieu_urbain_application_a_la_ville_de_Quito_Equater

Mohammadzadeh A., Tavakoli A., Valadan Zoej M.J. 2006. Road extraction based on fuzzy logic and mathematical morphology from pan-sharpened ikonos images. The Photogrammetric Record, 21(113), 44–60. https://doi.org/10.1111/j.1477-9730.2006.00353.x

MRE. 2019. Conférence Nationale sur les risques majeurs. Prise en charge de la problématique des inondations, Alger.

Ourabia S., Smara Y. 2016. A New Pansharpening Approach Based on Non Subsampled Contourlet Transform Using Enhanced PCA Applied to SPOT and ALSAT-2A Satellite Images. J. Indian. Soc. Remote Sens., 44, 665–674. https://doi.org/10.1007/s12524-016-0554-9

Pesaresi M., Benediktsson J.A. 2001. A new approach for the morphological segmentation of high-resolution satellite imagery. IEEE Transactions on Geoscience and Remote Sensing, 39(2), 309–320. https://doi.org/10.1109/36.905239

Pony O., Descombes X., Zerubia J. 2000. Classification d'images satellitaires hyperspectrales en zone rurale et périurbaine [Report, INRIA]. https://hal.inria.fr/inria-00072636

Puissant A., Weber C. 2003. Les images à très haute résolution, une source d'information géographique en milieu urbain?: État des lieux et perspectives. Espace géographique, 32(4), 345. https://doi.org/10.3917/eg.324.0345

Ranchin T., Wald L. 1995. Fusion d'images HRV de SPOT panchromatique et multibande à l'aide de la méthode ARSIS: Apports à la cartographie urbaine. Actes des 6 èmes journées scientifiques du Réseau Télédétection de l'AUPELF-UREF: Télédétection des milieux urbains et périurbains.

RGPH. 2008. Office National des Statistique.

Shan Yu, Berthod M., Giraudon G. 1999. Toward robust analysis of satellite images using map information-application to urban area detection. IEEE Transactions on Geoscience and Remote Sensing, 37(4), 1925–1939. https://doi.org/10.1109/36.774705

Shen P., Zhang J., Su Z. 2011. The Application of Remote Sensing in the Extraction of Urban Land Use Changes. Procedia Environmental Sciences, 10, 1589–1594. https://doi.org/10.1016/j.proenv.2011.09.252

Singh P.P, Garg R.D. 2012. Automatic Road Extraction from High Resolution Satellite Image using Adaptive Global Thresholding and Morphological Operations. Journal of the Indian Society of Remote Sensing, 41. https://doi.org/10.1007/s12524-012-0241-4

Song J., Gao S., Zhu Y., Ma C. 2019. A survey of remote sensing image classification based on CNNs. Big Earth Data, 3(3), 232–254. https://doi.org/10.1080/20964471.2019.1657720

Sparfel L., Gourmelon F., Le Berre I. 2008. Approche orientée-objet de l'occupation des sols enzone côtière. Revue Télédétection, 8, 4, 237–256.

Taubenböck H., Standfuß I., Wurm M., Krehl A., Siedentop S. 2017. Measuring morphological polycentricity. A comparative analysis of urban mass concentrations using remote sensing data. Computers, Environment and Urban Systems, 64, 42–56. https://doi.org/10.1016/j.compenvurbsys. 01.005 UNSD – Welcome to UNSD. Consulté 1 mars 2022. https://unstats.un.org/home/

Van der Kwast J., Canters F., Karssenberg D., Engelen G., Van de Voorde T., Uljee I., de Jong K. 2011. Remote sensing data assimilation in modeling urban dynamics: Objectives and methodology. Procedia Environmental Sciences, 7, 140–145. https://doi.org/10.1016/j.proenv.2011.07.025

Van der Linden S., Okujeni A., Canters F., Degerickx J., Heiden U., Hostert P., Priem F., Somers B., Thiel F. 2019. Imaging Spectroscopy of Urban Environments. Surveys in Geophysics, 40(3), 471–488. https://doi.org/10.1007/s10712-018-9486-y

Wang L., Shi C., Diao C., Ji W., Yin D. 2016. A survey of methods incorporating spatial information in image classification and spectral unmixing. International Journal of Remote Sensing, 37(16), 3870–3910. https://doi.org/10.1080/01431161.2016.1204032

Weng Q. 2012. Remote sensing of impervious surfaces in the urban areas: Requirements, methods, and trends. Remote Sensing of Environment, 117, 34–49. https://doi.org/10.1016/j.rse.2011.02.030

Zhang R., Lin X. 2010. Automatic road extraction based on local histogram and support vector data description classifier from very high resolution digital aerial. 2010 IEEE International Geoscience and Remote Sensing Symposium, 441–444. https://doi.org/10.1109/IGARSS.2010.5654117

Zhu Q., Zhong Y., Liu Y., Zhang L., Li D. 2018. A Deep-Local-Global Feature Fusion Framework for High Spatial Resolution Imagery Scene Classification. Remote Sensing, 10. https://doi.org/10.3390/rs10040568

PhD Tarek Medjadj
University of M'Sila, Algeria
Laboratory Smart City, Geomatics and Gouvernance
e-mail: tarek.madjedj@univ-msila.dz
ORCID: 0000-0002-1148-4413

PhD Hayet Ghribi
University of M'Sila, Algeria
Faculty of Math and Computer Sciences